Observations of Solar Wind Ion Charge Exchange in the Comet Halley Coma

S. A. FUSELIER AND E. G. SHELLEY

Lockheed Palo Alto Research Laboratory, Palo Alto, CA

B. E. GOLDSTEIN, R. GOLDSTEIN, AND M. NEUGEBAUER

Jet Propulsion Laboratory, California Institute of Technology, Pasadena, CA

W. -H. IP

Max-Planck-Institut für Aeronomie, Katlenberg-Lindau, FRG

H. BALSIGER

Physikalisches Institut, Universität Bern, Bern, Switzerland

H. RÈME

Centre d'Étude Spatiale des Rayonnements, Toulouse, France

Giotto Ion Mass Spectrometer/High Energy Range Spectrometer (IMS/HERS) observations of solar wind ions show charge exchange effects and solar wind compositional changes in the coma of comet Halley. As the comet was approached, the He^{2+} to proton density ratio increased until about 1 hour before closest approach after which time it decreased. Abrupt increases in this ratio were also observed in the beginning and near the end of the so-called Mystery Region (8.6 to 5.5×10^5 km from the comet along the spacecraft trajectory). These abrupt increases in the density ratio were well correlated with enhanced fluxes of keV electrons as measured by the Giotto plasma electron spectrometer. The general increase and then decrease of the He^{2+} to proton density ratio is quantitatively consistent with a combination of the addition of protons of cometary origin to the plasma and loss of plasma through charge exchange of protons and He^{2+}. In general agreement with the solar wind proton and He^{2+} observations, solar wind oxygen and carbon ions were observed to charge exchange from higher to lower charge states with decreasing distance to the comet. The more abrupt increases in the He^{2+} to proton and the He^{2+} to O^{6+} density ratios in the mystery region require a change in the solar wind ion composition in this region while the correlation with energetic electrons indicates processes associated with the comet.

INTRODUCTION

Soon after the spacecraft encounters with comet Halley, it was reported that a considerable amount of solar wind He^{2+} was charge exchanged to He^+ in the comet coma [*Balsiger et al.*, 1986; *Shelley et al.*, 1986]. Specifically, it was reported that inside the magnetic pile-up boundary (1.35×10^5 km from the nucleus along the Giotto trajectory), over 30% of the solar wind He^{2+} distribution was charge exchanged to He^+. This result

is illustrated in Figure 1, which shows the time profile of the ratio of M/Q=4 to He^{2+} + M/Q=4 densities. This time profile is similar to the one reported by *Shelley et al.* [1986, Figure 3] except that here, the contribution of cometary H_2^+ to the M/Q=2 mass peak has been removed (see *Fuselier et al.* [1988]). Because of the relatively high concentrations, the M/Q=4 mass peak is thought to contain mainly He^+ charge exchanged from solar wind He^{2+} near the comet (within 10^6 km from the nucleus), Figure 1 is expected to reasonably represent the fraction of charge exchanged solar wind He^{2+} as a function of distance from the comet along the Giotto spacecraft trajectory. This figure clearly shows that the charge exchanged fraction increased rather abruptly from <10% to over 40% after the magnetic pile-up boundary (MPB). (Model results will be discussed in a later section.)

Solar wind ion charge exchange with cometary neutrals in the comet coma was predicted prior to the spacecraft encounters with comet Halley [e.g., *Ip and Axford,* 1982]. However, charge exchange effects were expected to be important at distances less than about 10^4 km from the nucleus along the comet-sun line for a Halley-type comet [*Ip and Hsieh,* 1982]. The observations of significant charge exchange of solar wind He^{2+} at the magnetic pile-up boundary (Figure 1) correspond to a distance that is approximately an order of magnitude further from the comet nucleus than predicted.

Thus far, direct observations of charge exchange of solar wind ions have been limited to charge exchange of He^{2+} to He^+ in the comet Halley coma and possibly considerably tailward of the nucleus [Milhalov et al., 1987]. Although the charge exchange cross section for He^{2+} in H_2O is not known, it is probably on the order of 3×10^{-16} cm^2 for typical He^{2+} energies near the magnetic pile-up boundary [*Fite et al.*, 1962; *Koopman,* 1968]. Cross sections for other solar wind minor ions (e.g. O^{7+}, O^{6+}, etc.) in H_2O are also poorly known; however, they may be as much as an order of magnitude larger than that for He^{2+} and nearly equal to the cross section for H^+ in H_2O [*Koopman,* 1968; *Spjeldvik,* 1979]. Since such a large fraction of He^{2+} is charge exchanged in the vicinity of the

magnetic pile-up boundary (Figure 1), it follows that an even larger fraction of other solar wind ions should be charge exchanged in that region of the comet Halley coma. The larger cross sections of these other solar wind ions should also result in observable charge exchange effects further from the comet.

In this paper, we present observations of solar wind electrons and ions in the coma of comet Halley. These observations have potentially important consequences for charge exchange near the magnetic pile-up boundary and other locations throughout the comet Halley coma.

Ion observations in this paper were from the Giotto Ion Mass Spectrometer/High Energy Range Spectrometer (IMS/HERS) [*Balsiger et al.*, 1987]. This instrument cycled through four modes during the Halley encounter. The two modes of interest here measured the three dimensional velocity distributions of protons and solar wind ions with mass per charge (M/Q)=2 to 4 amu/e. Each individual mode required four seconds (one spacecraft spin) to complete an energy and angle scan and the modes were repeated sequentially every 16 seconds. The field-of-view of this instrument extended from 15 to 75° relative to the spacecraft spin axis (which was also approximately the spacecraft velocity vector relative to the comet) and ion energies from 10 eV/e to ~4 keV/e were measured.

For protons and He^{2+}, the moment calculations have been revised from previous work to include an estimate of the percentage of ions outside of the HERS field-of-view. In this procedure, the distribution was assumed to be gyrotropic in the plasma rest frame and the measured phase space density at each velocity and pitch angle was weighted by the inverse fraction of phase space sampled at that pitch angle. This procedure gave reliable estimates of the density as long as the bulk of the distribution was in the field-of-view. For protons and He^{2+}, the bulk of the distribution was in the HERS field-of-view from upstream of the shock (~10^6 km) to well inside the magnetic pile-up boundary (~10^4 km) [*Goldstein et al.*, 1991].

Electron observations in this paper were from the Electron Electrostatic Analyzer (RPA1-EESA) [*Rème et al.*, 1986]. This instrument measured a full 3-dimensional electron distribution from 10 eV to 30 keV every 2 seconds. Here, 4 second averages of these data were used.

OBSERVATIONS

Figure 2 shows the M/Q=2 to proton density ratio at 64 s resolution from 1830 UT to near closest approach to the comet. The distance to the comet along the spacecraft trajectory is shown above the density ratio profile and some of the major regions and boundaries are shown in the figure. The dashed line in this figure will be discussed in detail in the model section.

Upstream from the shock (1830-1922 UT), the M/Q=2 mass peak is dominated by solar wind He^{2+} and the M/Q=2 to proton density ratio shows rapid fluctuations ranging from 1.8 to 3.8%. These fluctuations are due in part to M/Q=2 counting statistics and the fact that the M/Q=2 ions were systematically measured 4 s before the protons. The magnitude of the fluctuations gives some indication of the uncertainty in the measured density ratio in this region. Downstream from the shock (1922 - 2400 UT), the average density ratio increases from about 2.5% to ~4% before decreasing near closest approach. More abrupt, longer lasting deviations are superposed on this trend with the two most notable deviations occurring at the beginning and near the end of the mystery region. After 2310 UT, both the M/Q=2 distribution and the proton distribution are contaminated by a substantial fraction of cometary ions. The M/Q=2 mass peak contains a significant fraction of cometary H_2^+ [*Fuselier et al.*, 1988] and the proton peak contains a significant fraction of cometary pick up protons. While it would be extremely difficult to separate the cometary and solar wind protons, the slight difference in the mass per charge of solar wind He^{2+} and cometary H_2^+ has been used to separate these two species [*Fuselier et al.*, 1988]. Using the density estimates for solar wind He^{2+} inside 2310 UT from Fuselier et

al., 5 min averages of the He^{2+} to proton density ratio are shown by the filled circles connected by the solid line in Figure 2. As can be seen, the He^{2+} to proton density ratio actually reaches a peak at about 2310 UT and decreases significantly thereafter.

In addition to protons and He^{2+}, the Giotto IMS/HERS sensor measured solar wind ions in the mass per charge range from 2 to 4. Figure 3 shows two mass spectra from M/Q=2 to 4 in the solar wind (upper panel) and near the comet (lower panel). Long averaging times were required to obtain good counting statistics for solar wind ions other than He^{2+}. Plotted is the countrate multiplied by $(M/Q)^4$ normalized to the peak countrate as a function of IMS/HERS mass channel. Error bars are one sigma based on counting statistics only. The Y-axis is roughly proportional to flux relative to the M/Q=2 ion flux (primarily He^{2+} in the solar wind and a mixture of He^{2+} and H_2^+ near the comet). In the solar wind spectrum, the O^{7+}, C^{5+}, and Ne^{8+} fluxes are about 0.5% of the solar wind He^{2+} flux while the O^{6+} and C^{4+} fluxes are about 1% of He^{2+}. In addition, there is a relatively small amount of M/Q=4 and slightly larger M/Q ions (probably of solar wind origin and consisting mainly of Si^{7+} with contributions from multiply charge iron ions).

The spectrum in the lower panel of Figure 3 near the comet shows considerable change from the solar wind spectrum. Solar wind O^{7+}, O^{6+}, and Ne^{8+} fluxes are all reduced relative to the M/Q=2 flux. The most dramatic change occurs in the M/Q=4 flux. It is now well above background at a few percent of the M/Q=2 flux.

Besides M/Q=2, the relatively good counting statistics for O^{6+}, the second most abundant solar wind minor ion, and M/Q=4 ions allow us to construct density profiles for these ion species with the time resolution needed to distinguish some features in the cometary coma. Figure 4 shows density profiles for these two ion species from the upstream solar wind to near closest approach. A variety of averaging intervals were used based on counting statistics of the individual ion species. For example, one hour averages were used in the solar wind and after 2200 UT and half hour averages were used between the shock and the end of the mystery region. Because of the 4 keV/e upper energy

per charge cutoff of the IMS/HERS detector, a fraction of the higher mass per charge solar wind ion distributions were outside the energy per charge range of the instrument. This energy per charge cutoff had the greatest effect on the M/Q=4 densities in the solar wind, where the solar wind velocity was relatively high. Because mass loading caused the solar wind velocity to decrease from about 400 km/s far from the comet to near zero near the comet, the upper energy per charge cutoff of the HERS detector had less effect on M/Q=4 densities closer to the comet. It is estimated that 47% of the distribution was above 4 keV/e from 1600-1700 UT, 20% from 1700-1800 UT and about 9% from 1800-1900 UT. After 1930 UT, the solar wind velocity had decreased enough so that a negligible amount of M/Q=4 solar wind ion distribution was above the 4 keV/e cutoff. For other solar wind ions, such as C^{4+} and O^{5+}, the upper energy per charge cutoff had much less effect on the density. It is estimated that less than 5% of the solar wind C^{4+} and O^{5+} distributions were above the 4 keV/e cutoff from 1600-1700 UT. This percentage decreased as the comet was approached.

Despite the long averaging times, some general trends can be seen in Figure 4. The O^{6+} density profile is similar to the proton and M/Q=2 density profiles [see *Goldstein et al.*, 1987; 1991]. In particular, it shows a factor of two increase in density between 2000 and 2200 UT associated with the mystery region. In contrast, The M/Q=4 density is at detection threshold ($\sim 10^{-3}$ cm^{-3}) in the solar wind and increases sharply after 2200 UT [see also, *Shelley et al.*, 1986].

Although the densities of other solar wind ions were extremely low, a general trend towards lower charge states was seen in the comet coma. Table 1 lists density ratios for Oxygen and Carbon charge states for the 2 hours prior to the crossing of the cometary bow shock ($\sim 10^6$ from the comet) and for the 2 hours before closest approach (~few x 10^5 km from the comet). Whereas the O^{7+} to O^{6+} density ratio decreased with decreasing distance to the comet, the O^{5+} to O^{6+} density ratio increased with decreasing distance. Also, the C^{4+} to C^{5+} ratio increased with decreasing distance to the comet. Although

the uncertainties are quite large, the general trend in Table 1 was toward lower charge states as the comet was approached.

CHARGE EXCHANGE

The observations in Figures 1 through 4 and Table 1 are qualitatively consistent with charge exchange of solar wind ions in the comet Halley coma. Figure 1 shows that He^{2+} was charge exchanged to He^{+} as the comet was approached. Figure 2 shows a general increase in the He^{2+} to proton density ratio as the comet was approached. This density ratio was affected by solar wind composition changes, addition of cometary protons, and charge exchange losses. The addition of comeatry protons would cause the He^{2+} to proton density ratio to decrease with decreasing distance to the comet. It is clear from Figure 2 that the presence of cometary protons does not have an effect before 2310 UT, when the density ratio began to decrease. The increase in the He^{2+} to proton density ratio from 1830 UT to 2310 UT could be due to a slow change in the solar wind composition (i.e., unrelated to the presence of the comet). However, the slow change in composition would not account for the increase in the M/Q = 4 ion density (interpreted as He^{+}) as the comet was approached (Figure 4). Charge exchange of He^{2+} and protons can account for the increase in the He^{2+} to proton density ratio in Figure 2 since, as discussed in the introduction, the charge exchange cross section for protons is believed to be ten times higher than that for He^{2+}. Charge exchange of He^{2+} to He^{+} also accounts for the increase in the M/Q=4 ion density as the comet was approached. Although there are several other possible sources for the M/Q=4 mass peak (see Figure 3), the total density of the solar wind ions between M/Q=2 to 4 is only a few percent of the He^{2+} density. Therefore, these ions cannot contribute significantly to the M/Q=4 ion density near the comet and the major contribution to the M/Q=4 mass peak appears to be He^{+} charge exchanged from solar wind He^{2+} [see also, *Shelley et al.*, 1986]. Superposed on the charge exchange loss of

He^{2+} and protons are possible solar wind composition changes (for example from 2120 to 2150 UT in Figure 1) which will be discussed in more detail in the next two sections.

Figure 3 and Table 1 are also consistent with charge exchange as the comet was approached. In Figure 3, there is evidence for a loss of solar wind minor ions such as O^{7+} and Ne^{8+} close to the comet. In Table 1, there is a general trend to lower oxygen and carbon charge states as the comet was approached. Since all charge states of solar wind oxygen have approximately the same charge exchange cross section [*Spjeldvik*, 1979], the general trend to lower charge states indicates that multiply charged ions undergo charge exchange as the solar wind approaches the comet.

MODEL FOR PROTON AND He^{2+} CHARGE EXCHANGE

Unfortunately, the very low densities of the solar wind minor ions between M/Q=2 and 4 allow only a qualitative comparison with predictions from solar wind ion charge exchange. However, the proton, M/Q=2, and M/Q=4 densities are large enough to allow some quantitative comparison with predictions from solar wind ion charge exchange. Comparison between the observations and a simple model for the solar wind interaction have already been made [*Shelley et al.*, 1986]. Shelley et al. concluded that the helium observations in the comet coma were inconsistent with present models of the solar wind interaction with the comet. They suggested that model results and observations would be in better agreement if the He^{2+} to He^{+} charge exchange cross section in H_2O was substantially larger than the $\sim 3 \times 10^{-16}$ cm^2 assumed in their model and/or if the flow field in the comet coma was substantially different than assumed in their model.

Given a cometary flow model, the ratio of the He^{2+} and proton densities can be determined along the Giotto trajectory. This ratio will depend on the ratio of the charge exchange cross sections of He^{2+} and protons and on the production rate of cometary H^{+} from H_2O. Since the proton charge exchange cross section in H_2O at the energies of interest here is reasonably well known and the production of H^{+} can be modeled, the profile of the

He^{2+} to proton density ratio is a function of the He^{2+} charge exchange cross section. In this section, we use a cometary flow model to predict the He^{2+} to proton density ratio and compare this prediction to the observations. Through this comparison, we estimate the charge exchange cross section for He^{2+} in H_2O.

The model charge exchange calculations were made using the procedure outlined in *Ip* [1989]. The MHD flow dynamics of the comet-solar wind interaction were separated from the photochemistry and the charge exchange process. In doing this, the continuity equation

$$\frac{1}{A}\frac{d}{ds}(n_j v_j A) = q_j - s_j \tag{1}$$

for the j^{th} species can be integrated. Here, v_j is the flow velocity along the stream line, n_j is the number density, q_j is the production rate, s_j is the loss rate, and A is the cross section of the stream tube. The flow field model determines the values of v_j for each stream line and the cross section of the stream line. Here, we use the Fedder et al. 2-D flow model [*Fedder et al.*, 1986].

To compute the net production rate for cometary H^+ (q_H-s_H in Equation 1), we assume a coma model of water vapor and its photodissociation fragments (OH, O, and H). The production rate for hydrogen ions is then given by,

$$\dot{n}(H^+) = n(H)\,(1/t_i + \sum_j n_j \sigma_j(H) < v_j >) \tag{2}$$

Here the ionization time (t_i), which includes photoionization and charge exchange with solar wind protons, is assumed to be 10^6 seconds. The cross section $\sigma_j(H)$ in the second term refers to the interaction between H^+ and the neutral gas and $<v_j>$ is the root-mean-square of the plasma flow speed v_p and the thermal speed (δv_j) of the j^{th} species.

The loss term in (1) is dominated by the charge exchange process. Although charge exchange cross sections for different reactions should vary with the flow speed, in the present approximation we assume the the charge exchange rate for protons is constant with energy.

The dashed line in Figure 2 shows the results from the model. In the model, the initial density ratio was 2.5%, the He^{2+} charge exchange cross section was $\sigma = 3\times10^{-16}$ cm^2, and the H^+ charge exchange cross section was 5×10^{-15} cm^2. The general trend of the observed density ratio is reproduced, indicating that the charge exchange cross section for He^{2+} is about a factor of 10 lower than that for H^+. Increasing the He^{2+} charge exchange cross section by a factor of 10 would result in a He^{2+} to proton density ratio that neither has an initial increase with decreasing distance nor has a decrease in the last hour before closest approach.

Since the densities are computed individually in the model, the He^+ to total Helium ion density ratio can be directly compared with the observations in Figure 1. The percent charge exchanged He^{2+} predicted from the model (solid line connected by x's in Figure 1) is clearly in good agreement with the observations up to the magnetic pile-up boundary. This is again consistent with a He^{2+} charge exchange cross section of $\sim3\times10^{-16}$ cm^2 for this region. After the magnetic pile-up boundary, the predicted percentage is about a factor of 4 below the observed percentage.

Thus, while the general trend in Figures 1 and 2 are reproduced with the expected cross sections, the model underestimates the density ratio in the mystery region and near the magnetic pile-up boundary. and it also underestimates the percent charge exchanged He^{2+} near the magnetic pile-up boundary. In the next section, we address the discrepancy between observations and predictions in the mystery region by considering why the density ratio changes rather abruptly. The deviation between observations and predictions is left for the final discussion secion.

MYSTERY REGION

The mystery region is a region of increased density, increased flow speed, decreased ion temperature, and increased electron temperature relative to the rest of the region downstream from the Giotto bowshock crossing [*Goldstein et al.*, 1986; *Rème et al.*, 1986; *Rème*, 1990]. Figure 2 also shows that the M/Q=2 to proton density ratio deviates from its relatively smooth, increasing trend in this region. In this section, we will discuss the possible origins of these deviations and other properties of the mystery region.

Figure 5 shows the density profiles for electrons from 10 eV to 3.5 keV, protons, M/Q=2 ions (primarily solar wind He^{2+}), solar wind O^{6+}, and electrons from 0.8 to 3.5 keV. The proton and electron density profiles in the top two panels show both qualitative and quantitative agreement throughout this time interval. The mystery region extends from the sharp density increase at 2022 UT to the sharp decrease in the M/Q=2 ion density and the 0.8 to 3.5 keV electron density at 2152 UT.

The horizontal bars in Figure 5 show the time intervals when the M/Q=2 to proton density ratio in Figure 2 deviated from its smooth trend. Of particular interest is the interval from 2115 to 2150 UT. As can be seen in Figure 5 at 2120 UT, the increase in the M/Q=2 to proton density ratio in Figure 2 is associated with a drop in both the electron and proton number densities. The M/Q=2 number density did not decrease from 2115 to 2125 UT, in fact, it increased somewhat. The net result was an abrupt increase in the M/Q=2 to proton density ratio. It is also interesting to note that the changes in the M/Q=2 to proton density ratio in the period from 2115 to 2150 UT are associated with a decrease in the solar wind O^{6+} density and an increase in the electron density above 800 eV (see the bottom two panels in Figure 5). The half hour averages of the O^{6+} density do not allow us to determine if a similar decrease in that density is associated with the first interval of increased M/Q=2 to proton density ratio from 2013 to 2021 UT. However,

it is clear that the increase in the M/Q=2 to proton density ratio is associated with increased electron density above 800 eV from 2037 to 2105 UT. The energetic electron density increases in the mystery region are unique. From the bow shock to the mystery region and after the mystery region to closest approach, the energetic electron density was $\sim 3\text{-}4 \times 10^{-4}$ cm^{-3} (see Figure 5 from 2000 to 2040 UT and *Rème et al.* [1986]).

DISCUSSION

In most regions of the comet Halley coma, we have attempted to interpret the IMS/HERS observations in terms of charge exchange with cometary neutrals. The increase in the He^+ density with decreasing distance to the comet in Figure 1, the general increasing M/Q=2 to H^+ density ratio in Figure 2, and the trend to lower charge states for multiply charged Oxygen and Carbon in Table 1 are all considered as evidence for this charge exchange process.

While we can find substantial qualitative evidence for charge exchange in the comet Halley coma, quantitative comparisons between the observations and predictions from cometary models is clearly lacking in the mystery region and the region near and inside the magnetic pile-up boundary.

To the properties of the mystery region that have been known previously [e.g., *Goldstein et al.*, 1986; *Rème et al.*, 1990], we add that there are solar wind composition changes in parts of this region. The He^{2+} to proton density ratio shows two deviations in its increasing trend in this region (see Figure 2). The second of these deviations occurs within the last 30 minutes of the mystery region and is associated with a decrease in the proton density and a possible slight increase in the M/Q=2 density (see Figure 5). Also, it is associated with a decrease in the O^{6+} density and the largest fluxes of energetic electrons observed during the encounter.

The general increase in all solar wind ion densities and the change in the He^{2+} to proton density ratio are strong indicators that the mystery region is dominated by solar

wind plasma with different characteristics from the plasma in other parts of the coma. While it is tempting to interpret this region as simply a separate solar wind plasma that has convected into the Halley coma, the observation of keV electrons in this region indicates that there is also an additional interaction related to the presence of the comet. It is also interesting to note that the second increase in the He^{2+} to proton density ratio (from 2115 to 2150 UT in Figure 5) results primarily from the decrease in the proton density and there is a simultaneous decrease in the O^{6+} density. As pointed out in the introduction, H^+ and O^{6+} both have charge exchange cross sections that are an order of magnitude larger than that for He^{2+}. This observation suggests that enhanced charge exchange may be occurring in the parts of the mystery region where the He^{2+} to H^+ density ratio is elevated and keV electrons are present. The possible causes of this enhanced charge exchange and the relation, if any, with the keV electrons are not known at this time. Also, it has been noted that the transition from the mystery region back into lower density plasma (at 2150 UT in Figure 5) may have been seen by other spacecraft that encountered comet Halley and by the Iternational Cometary Explorer (ICE) spacecraft at comet Giacobini-Zinner [*Rème et al.*, 1986; *Rème*, 1990].

Thus, while the observations in Figures 2 and 5 indicate that the mystery region is likely a separate solar wind plasma that has convected into comet coma, some of the features in this region and possibly its boundaries indicate that additional and different interactions between this plasma and the comet coma are taking place.

Another important region where the cometary models fail to predict the amount of charge exchange is the region from 2310 UT to closest approach, or the region near and inside the magnetic pile-up boundary. Figure 1 shows that the amount of charge exchanged He^{2+} to He^+ increases dramatically across the magnetic pile-up boundary. This amount is much larger than that predicted by previous models [*Shelley et al.*, 1986] and by the model used in this paper. In addition, the predicted He^{2+} to H^+ density ratio is clearly too low (Figure 2).

The difference between the predicted and observed density ratios indicates that either there is too little He^{2+} or too much H^+ present in the vicinity of the magnetic pile-up boundary. As pointed out by *Shelley et al.* [1986] the sharp increase in the percent charge exchanged He^{2+} at the Magnetic Pile-up Boundary (Figure 1) is not the result of a rapid increase in the He^+ density but a rapid decrease in the He^{2+} density. These results taken together suggest that the charge exchange of He^{2+} relative to H^+ is underestimated in the cometary models. An overestimate of the the production of cometary H^+ could also help explain the differences between predictions and observations in Figure 2 in the vicinity of the Magnetic Pile-up Boundary but obviously do not affect the results in Figure 1.

A possibility already discussed by *Shelley et al.* [1986] is that the He^{2+} cross section could be about a factor of 3 to 10 times larger than the 3×10^{-16} cm^2 value used in the models. This is clearly not the case prior to 2310 UT, where the predicted density ratio using this cross section agrees well with the observations. One possibility is that the cross section for He^{2+} increases with decreasing energy faster than that for H^+. (The H^+ cross section has been shown to increase with decreasing energy for energies below 100 eV [*Koopman* 1968].) Armed with such a free parameter, the density ratio profile in Figure 2 could be reproduced exactly, but the understanding of the density ratio decrease after 2310 UT would not be improved. Also, this possibility would not explain the rather abrupt increase in the percent charge exchanged He^{2+} in Figure 1 because the He^{2+} flow velocity decreases smoothly across the magnetic pile-up boundary and the thermal speed does not change at all across this boundary [*Fuselier et al.*, 1987]. One thing that does change rather abruptly in the vicinity of the magnetic pile-up boundary is the flow direction [*Fuselier et al.*, 1987].

It is possible that a combination of rapid slowing and deflection of the solar wind plasma incident along the sun-comet line, followed by a re-acceleration along the flanks of the comet could explain both the large amount of charge exchange and the relatively

smooth velocity profile observed by Giotto [*Shelley et al.*, 1986; *Wallis*, 1990]. However, the present computer models cannot be used to predict such a possibility. Thus, we must conclude that present computer models allow us to qualitatively understand the charge exchange of solar wind ions in the outer reaches of the coma and help to distinguish real charge exchange effects from changes in the solar wind composition (for example in the mystery region). The quantitative understanding of the observations of charge exchange in the inner coma (i.e. in the region just before and inside the magnetic pile-up boundary in Figures 1 and 2) remains poor.

Acknowledgments. The authors acknowledge the contributions of the entire IMS team. Research at Lockheed was funded by NASA under contract NAS5-4336. Work at the Centre d'Ètude Spatiale des Rayonnements was supported by CNES under grant number 1212.

REFERENCES

Balsiger, H., K. Altwegg, F. Buhler, J. Geiss, A. G. Ghielmetti, B. E. Goldstein, R. Goldstein, W. T. Huntress, W.-H. Ip, A. J. Lazarus, A. Meier, M. Neugebauer, U. Rettenmund, H. Rosenbauer, R. Schwenn, R. D. Sharp, E. G. Shelley, E. Ungstrup, and D. T. Young, Ion composition and dynamics at comet Halley, *Nature, 321*, 330-334, 1986.

Balsiger, H., K. Altwegg, J. Benson, F. Buhler, J. Fischer, J. Geiss, B. E. Goldstein, R. Goldstein, P. Hemmerich, G. Kulzer, A. J. Lazarus, A. Meier, M. Neugebauer, U. Rettenmund, H. Rosenbauer, K. Sager, T. Sanders, R. Schwenn, E. G. Shelley, D. Simpson, and D. T. Young, The ion mass spectrometer on Giotto, *J. Phys. E: Sci. Instrum., 20*, 759-767, 1987.

Fedder, J. A., J. G. Lyon, J. L. Giuliani Jr., ,*EOS Trans. AGU, 67*, 17, 1986.

Fuselier, S. A., E. G. Shelley, H. Balsiger, J. Geiss, B. E. Goldstein, R. Goldstein, W. -H. Ip, Cometary H_2^+ and solar wind He^{2+} dynamics across the Halley cometopause, *Geophys. Res. Lett., 15*, 549-552, 1988.

Goldstein, B. E., M. Neugebauer, H. Balsiger, J. Drake, S. A. Fuselier, R. Goldstein, W.-I. Ip, U. Rettenmund, H. Rosenbauer, R. Schwenn, and E. G. Shelley, Giotto-IMS observations of ion flow velocities and temperatures outside the contact surface of comet Halley, Proceedings of the 20th ESLAB Symposium on the Exploration of Halley's Comet, *ESA SP-250, 1*, 229-233, 1986, *Astron. and Astrophys., 187*, 174-178, 1987.

Goldstein, B. E., R. Goldstein, M. Neugebauer, S. A. Fuselier, E. G. Shelley, H. Balsiger, G. Kettmann, W.-H. Ip, H. Rosenbauer, and R. Schwenn, Observations of plasma parameters in the coma of P/Halley by the Giotto ion mass spectrometer, *J. Geophys. Res.*, submitted, 1991.

Ip, W.-H., On charge exchange effect in the vicinity of the cometopause of comet Halley, *Astrophys. J., in press*, 1989.

Ip, W.-H., and K. C. Hsieh, Production of energetic neutrals in cometary comae via solar wind interaction, in *Cometary Exploration I*, ed. T. I. Gombosi, Hungarian Academy of Sciences, 265-270, 1982.

Ip, W.-H., and W. I. Axford, Theories of physical processes in the cometary comae and ion tails, in *Comets*, ed. L. L. Wilkening, The University of Arizona Press, Tucson, 588-634, 1982.

Koopman, D. W., Light ion charge exchange in atmospheric gases, *Phys. Rev., 166*, 57-62, 1968.

Mihalov, J. D., H. R. Collard, D. S. Intriligator, and A. Barnes, Observations by Pioneer 7 of He^+ in the distant coma of Halley's comet, *Icarus, 71*, 192-197, 1987.

Rème, H., Cometary plasma observations between the shock and the contact surface, *J. Geophys. Res.*, in press, 1990.

Rème, H., F. Cotin, A. Cros, J. L. Médale, J. A Sauvaud, C. d'Uston, A. Korth, A. K. Richter, A. Loidl, K. A. Anderson, C. W. Carlson, D. W. Curtis, R. P. Lin, and D. A. Mendis, The Giotto RPA-Copernic plasma experiment, *ESA SP-177*, 33-52, 1986.

Rème, H., J. A Sauvaud, C. d'Uston, A. Cros, K. A. Anderson, C. W. Carlson, D. W. Curtis, R. P. Lin, A. Korth, A. K. Richter, and D. A. Mendis, General Features of the comet Halley - solar wind interaction from plasma measurements, *ESA SP-250, 1,* 29-34, 1986, *Astron. and Astrophys., 187,* 33-38, 1987.

Shelley, E. G., S. A. Fuselier, J. F. Drake, W.-I. Ip, H. Balsiger, B. E. Goldstein, R. Goldstein, M. Neugebauer, Charge exchange of solar wind ions in the comet Halley coma, Proceedings of the 20th ESLAB Symposium on the Exploration of Halley's Comet, *ESA SP-250, 1,* 285-289, 1986, *Astron. and Astrophys., 187,* 304-306, 1987.

Spjeldvik, W. N., Expected charge states of energetic ions in the magnetosphere, *Space Science Reviews, 23,* 499-538, 1979.

Wallis, M. K., Charge exchange regime in the plasma flow as source of cometosheath and Halley's plasma tail, *J. Geophys. Res.,* in press, 1990.

Table 1. Solar wind Oxygen and Carbon density ratios

Time (UT)	O^{7+}/O^{6+}	O^{5+}/O^{6+}	C^{4+}/C^{5+}
1705-1913	0.35±0.14	0.24±0.20	0.42±0.44
2200-2400	0.17±0.31	0.59±0.81	0.74±0.92

Fig. 1. Observed (+'s) and modeled (x's) M/Q=4 to He^{2+} + M/Q=4 density ratio versus distance from the comet along the Giotto trajectory. The abrupt increase at the magnetic pile-up boundary (MPB) is interpreted as a large increase in the percent He^{2+} charge exchange to He^{+}.

Fig. 2. M/Q=2 to H^{+} density ratio versus time or distance from the comet (solid line). The filled circles connected by the solid line are the ratios after the cometary H_2^{+} contribution to the M/Q=2 mass peak is removed. The Dashed line show a fit to the observed ratio from the charge exchange model.

Fig. 3. Mass spectra from M/Q=2 to 4 far from the comet (upper panel) and near the comet (lower panel). The vertical axis is proportional to the flux normalized by the He^{2+} flux. Near the comet, the relative fluxes of all multiply charged solar wind species are reduced except for M/Q=4 when compared to the mass spectrum further away.

Fig. 4. Densities versus time for M/Q=4 ions (dashed line) and solar wind O^{6+} (solid line).

Fig. 5. Electron, proton, He^{2+}, O^{6+}, and electron $\geq$1 keV densities for a time period centered on the mystery region. The bars in the figure identify the intervals when the He^{2+} to H^{+} density ratio in Figure 2 are elevated. These intervals are correlated with enhanced energetic electron flux. The second interval is also correlated with a decrease in the H^{+} and O^{6+} densities.

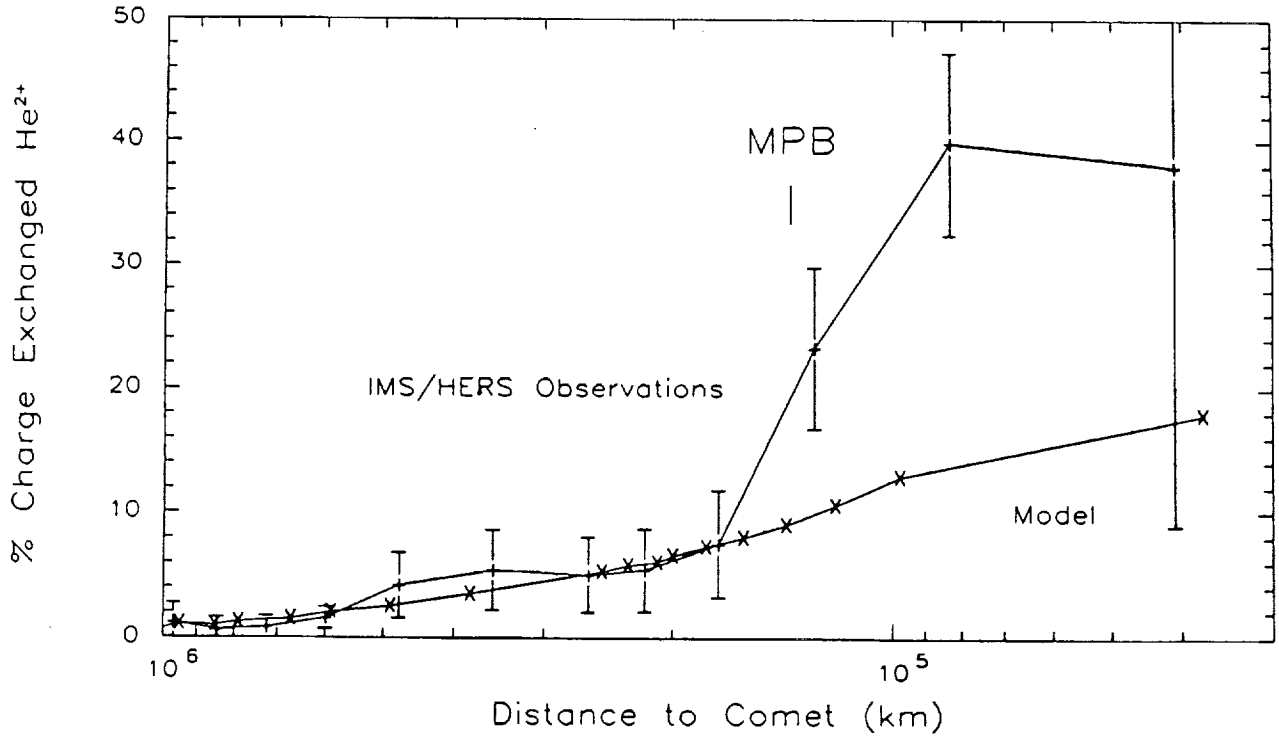
50
40
30
20
10
0
% Charge Exchanged He^{2+}
MPB
IMS/HERS Observations
Model
10^6
10^5
Distance to Comet (km)

Figure 1

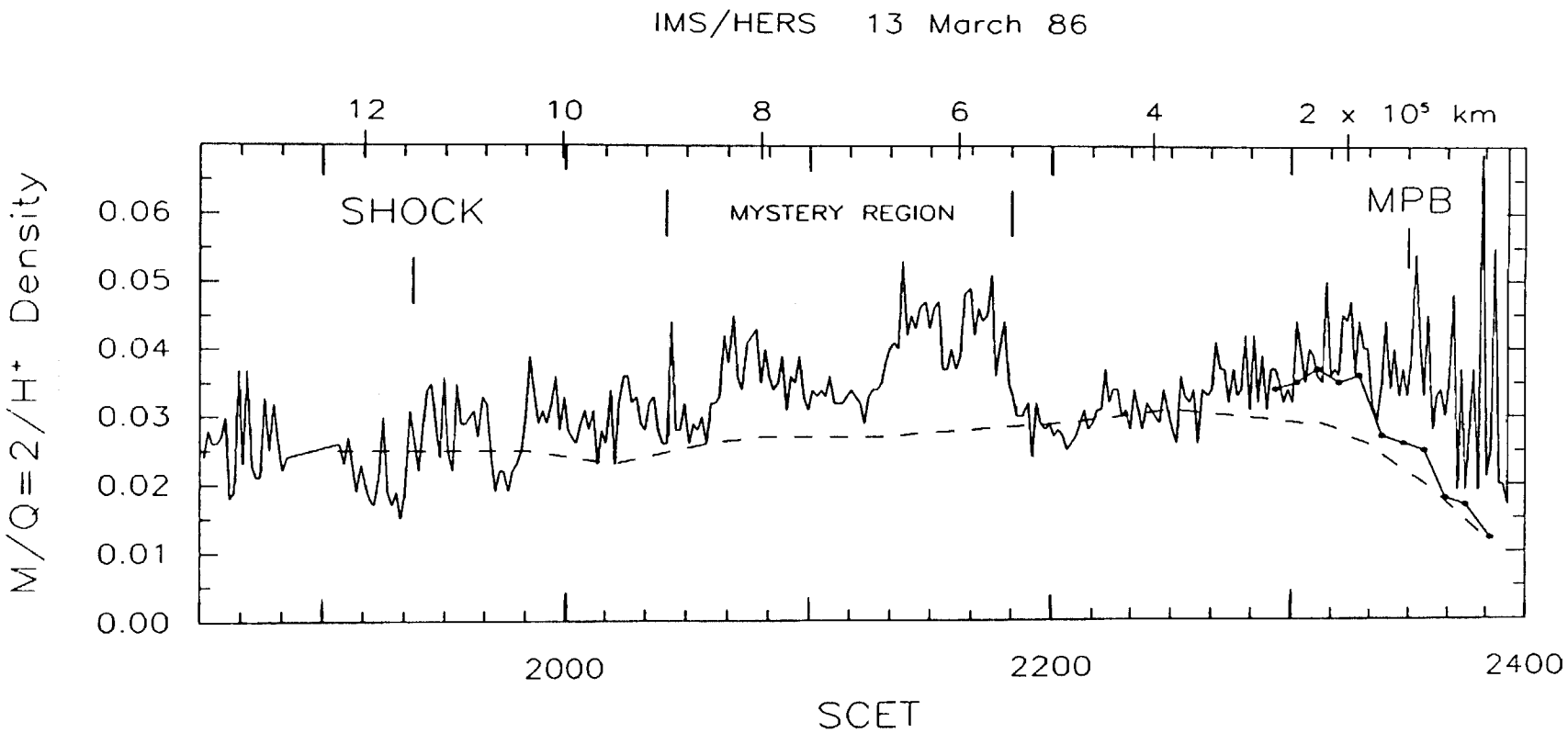
IMS/HERS 13 March 86
12
10
8
6
4
2 x 10⁵ km
SHOCK
MYSTERY REGION
MPB
M/Q=2/H⁺ Density
0.06
0.05
0.04
0.03
0.02
0.01
0.00
2000
2200
2400
SCET

Figure 2

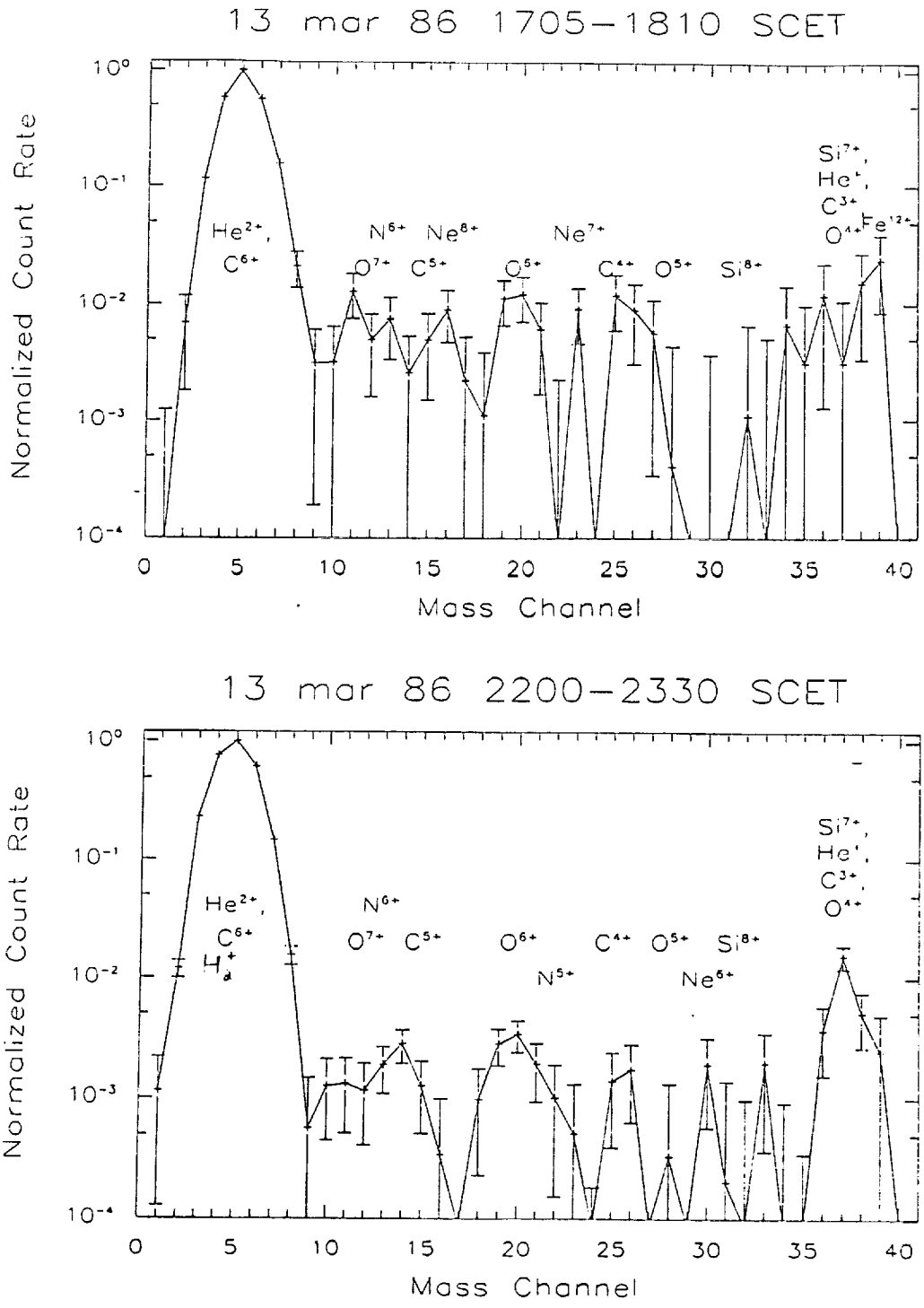
13 mar 86 1705–1810 SCET
Normalized Count Rate
Mass Channel
He2+, C6+
N6+ Ne8+
O7+ C5+
O5+
Ne7+
C4+ O5+
Si8+
Si7+, He+, C3+ O4+ Fe12+
13 mar 86 2200–2330 SCET
Normalized Count Rate
Mass Channel
He2+, C6+ H2+
N6+
O7+ C5+
O6+
N5+
C4+ O5+ Si8+
Ne6+
Si7+, He+, C3+, O4+

Figure 3

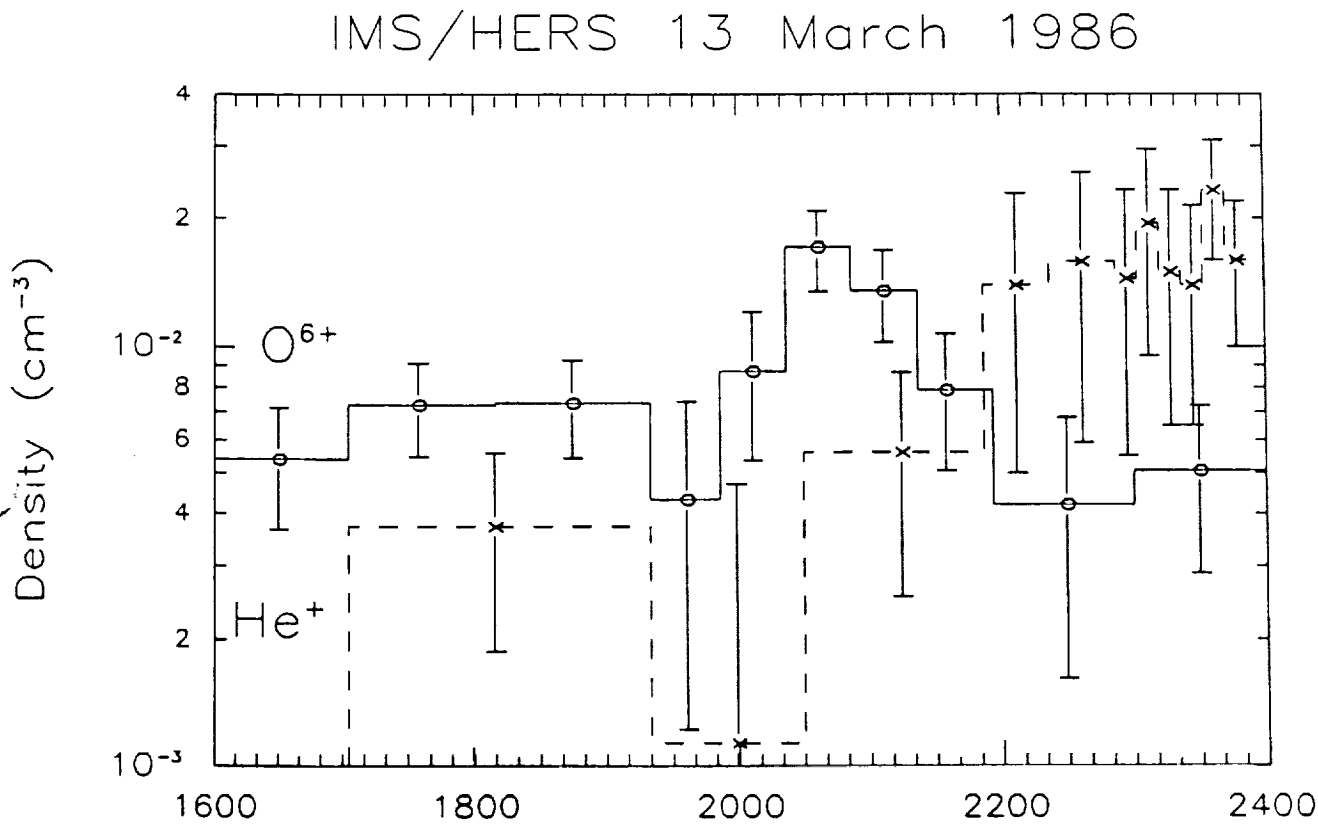
IMS/HERS 13 March 1986
Density (cm⁻³)
4
2
10⁻²
8
6
4
2
10⁻³
O⁶⁺
He⁺
1600
1800
2000
2200
2400

Figure 4

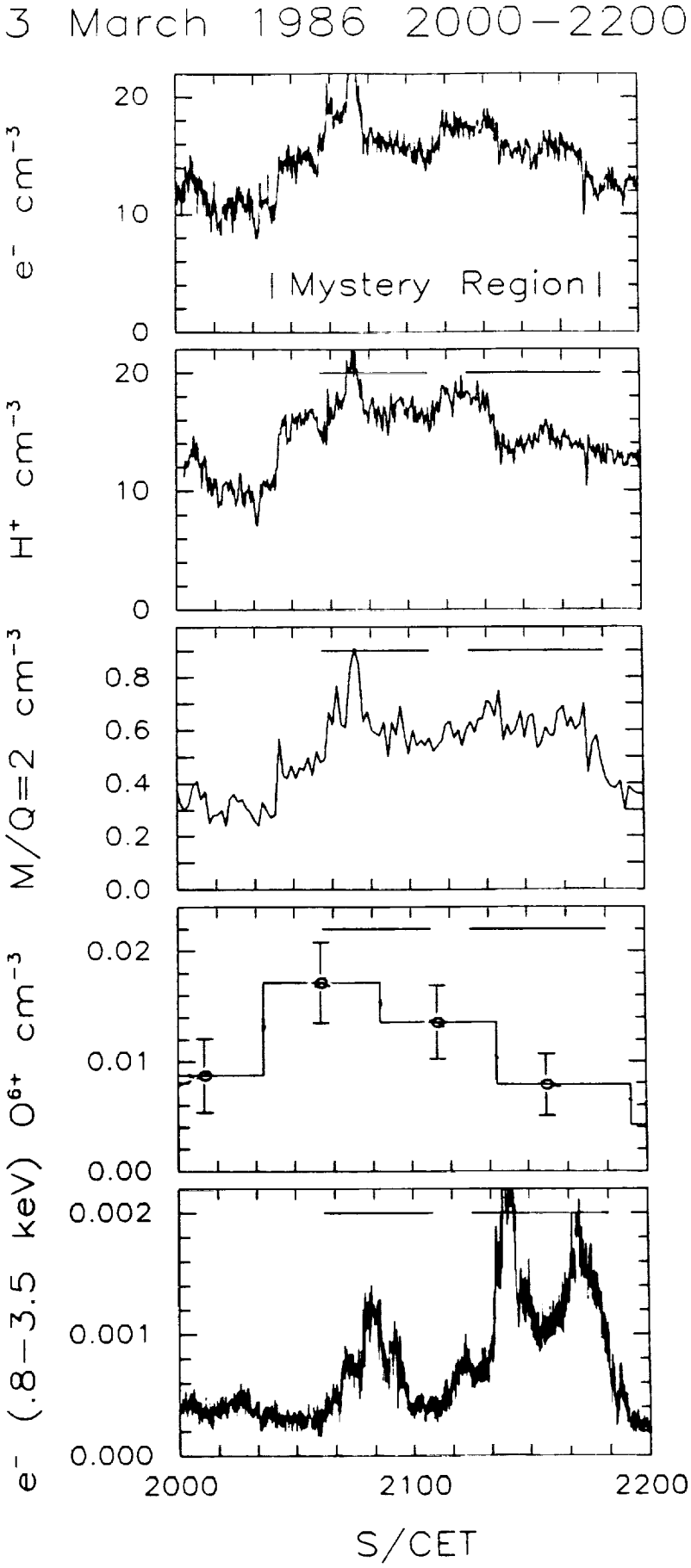
13 March 1986 2000–2200 SCET
e⁻ cm⁻³
20
10
0
Mystery Region
H⁺ cm⁻³
20
10
0
M/Q=2 cm⁻³
0.8
0.6
0.4
0.2
0.0
O⁶⁺ cm⁻³
0.02
0.01
0.00
e⁻ (.8–3.5 keV)
0.002
0.001
0.000
2000
2100
2200
S/CET

Figure 5